

Assembly of Tim9 and Tim10 into a Functional Chaperone*

Received for publication, March 8, 2002, and in revised form, July 1, 2002
Published, JBC Papers in Press, July 22, 2002, DOI 10.1074/jbc.M202310200

Sarah Vial‡§, Hui Lu‡, Scott Allen‡¶, Peter Savory‡, David Thornton||, John Sheehan||**,
and Kostas Tokatlidis‡ ‡§§

From the ‡School of Biological Sciences and ||The Wellcome Trust Centre for Cell Matrix Research,
University of Manchester, Manchester M13 9PT, United Kingdom and the §§Department of Chemistry,
University of Crete and Institute of Molecular Biology and Biotechnology, Heraklion, Greece

The TIM10 complex is localized in the mitochondrial intermembrane space and mediates insertion of hydrophobic proteins at the inner membrane. We have characterized TIM10 assembly and analyzed the structural properties of its subunits, Tim9 and Tim10. Both proteins are α -helical with a protease-resistant central domain, and each self-associates to form mainly dimers and trimers in solution. Tim9 and Tim10 bound to one another with submicromolar affinity in equimolar amounts and assembled in a stable, significantly extended complex that was indistinguishable from the native mitochondrial TIM10 complex. Importantly, the reconstituted TIM10 complex is functional because it bound to the physiological substrate ADP/ATP carrier and displayed chaperone activity in refolding the model substrate firefly luciferase. These data demonstrate that the individual subunits can exist as independent, dynamically self-associating proteins. Assembly into the thermodynamically stable hexameric complex is necessary for the TIM10 chaperone function.

Almost all mitochondrial proteins are synthesized in the cytosol and then imported into the organelle in a process that is dictated by each protein's sequence and that is ensured by the function of specialized translocation machineries in the organelle (1–4). Most import and intramitochondrial sorting pathways are variants of the general “matrix pathway,” first described in detail for matrix-targeted proteins (1–4). In this pathway, a mitochondrial precursor, which is usually synthesized with an N-terminal, positively charged, amphiphilic presequence, first interacts with cytosolic chaperones. It is then bound by a hetero-oligomeric receptor system on the surface of mitochondria in a process that requires ATP hydrolysis in the cytosol. The polypeptide chain is then transported across two hetero-oligomeric protein import channels, the TOM complex in the outer membrane and the TIM23 complex in the inner

membrane. Translocation is completed by the electrophoretic function of the electrochemical potential across the inner membrane and the ATP-powered import motor attached to the inner side of the TIM23 complex. In this pathway, targeting of the polypeptide chain from one complex to the other appears to be directed by increasing avidity of the positive presequence for a series of acidic receptor domains (“acid chain hypothesis”) (5–9).

The structural basis of this mechanism is becoming increasingly clear through advances in understanding the structural characteristics of key components at different steps of this pathway. First, the solution structure (determined by NMR) of the cytosolic part of the Tom20 receptor in complex with a synthetic presequence has been solved (10, 11): this showed that the presequence is in α -helical conformation and that binding between the receptor and the presequence involves hydrophobic stretches. Second, the existence of a hydrophilic channel of TOM40 as the outer membrane import pore and its dynamic behavior have been established (12–16). Third, Tim23 was shown to form a cation-selective, membrane potential-dependent channel in the inner membrane with specificity for presequences (17, 18). Finally, the crystal structure of the mitochondrial processing peptidase in complex with synthetic import signals has been determined (19). This revealed that the recognition of the presequence is context-specific: in the final step of import, the presequence is recognized by the matrix protease in extended conformation, unlike the helical motif it adopts in the vicinity of the import machinery components. In this general import pathway, components in the mitochondrial intermembrane space (IMS)¹ are conspicuously absent. This could be explained by the fact that the TOM and TIM channels are thought to be juxtaposed at dynamic “contact sites” drawn together by the presequence, thereby “shielding” the precursor in a “continuous” conduit to pass from one membrane to the other.

However, the situation is quite different for metabolite carriers of the inner membrane that lack a presequence and contain internal targeting sequences instead (20–22). These precursors require not only a translocation machinery in the outer and inner membranes, but, quite uniquely, a separate soluble intermembrane space complex as well (2, 23–26). The carrier proteins interact with a specific receptor system in the outer membrane and are then passed onto the TOM40 channel (27). Following that, they are inserted at the inner membrane in a membrane potential-dependent manner (22, 28) by the TIM22 complex (24, 29), a machinery whose major subunit and a channel-forming component is Tim22 (30), a protein homolo-

* This work was supported in part by the Wellcome Trust and a Medical Research Council cooperative group grant (to K. T. and J. S.) and by the UK Medical Research Council and the UK Biotechnology and Biological Sciences Research Council (to K. T.). The costs of publication of this article were defrayed in part by the payment of page charges. This article must therefore be hereby marked “advertisement” in accordance with 18 U.S.C. Section 1734 solely to indicate this fact.

§ Supported by a European Union Marie Curie postdoctoral fellowship.

¶ Supported by a Biotechnology and Biological Sciences Research Council studentship.

** Present address: Thurston Bowles Bldg., University of North Carolina, Chapel Hill, NC 27514.

‡‡ Lister Institute Research Fellow. To whom correspondence should be addressed: School of Biological Sciences, University of Manchester, 2.205 Stopford Bldg., Oxford Rd., Manchester M13 9PT, UK. Tel.: 44-161-275-5687; Fax: 44-161-275-5082; E-mail: tokatlidis@man.ac.uk.

¹ The abbreviations used are: IMS, intermembrane space; AAC, ADP/ATP carrier; GST, glutathione S-transferase; DTT, dithiothreitol; MOPS, 4-morpholinepropanesulfonic acid; BSA, bovine serum albumin.

gous to Tim23 (29). Passage across the intermembrane space is specifically mediated by the TIM10 complex. TIM10 is exclusively made of Tim9 and Tim10 (31), two homologous, zinc-binding proteins (25, 26). The TIM10 complex facilitates transfer of carriers from the outer membrane to the outer surface of the inner membrane. Then, Tim12, a protein homologous to Tim9 and Tim10 and peripherally attached to the membrane, takes over and facilitates insertion into the membrane in the context of the TIM22 complex, which contains all of Tim12, trace amounts of Tim9 and Tim10, Tim54, and Tim18 (25, 26, 32–34). Despite their sequence homology, the TIM10 complex is in large excess over Tim12 and the TIM22 complex. To account for the different localization and relative amounts of the two complexes, we have proposed that this is a “two-affinity system” (35). First, the TIM10 complex functions as a low affinity chaperone-like system, interacting with a large number of precursors, which could explain why it is needed in large amounts. Subsequently, the TIM22 system, which is a more specialized insertion machinery, interacts with high affinity with the hydrophobic precursors (2, 31, 36, 37).

We have recently shown by coexpression in *Escherichia coli* that Tim9 and Tim10 are the only two mitochondrial proteins necessary and sufficient to form the TIM10 complex (31). The functionality of the recombinant complex *in organelle* was shown by restoring AAC import in TIM10-deficient mitochondria upon replenishing them with Tim9 and Tim10 (31). Here, we report the *in vitro* reconstitution of the TIM10 complex by individually purified subunits. The subunits dynamically self-associate in α -helical structures; and upon assembly, they form a complex identical to the IMS complex. We structurally characterized the two proteins and their assembly and determined their binding affinity to be very high (K_d at submicromolar range). The reconstituted complex was shown to be active by binding to AAC *in vitro* and showed a chaperone activity in refolding denatured luciferase.

EXPERIMENTAL PROCEDURES

Purification of Tim10 and Tim9 from *E. coli*

Tim10—Strain BL21-Codon Plus (Stratagene) containing a plasmid expressing GST-Tim10 was grown in 1 liter of LB medium supplemented with ampicillin (0.1 mg/ml) at 30 °C to $A_{600\text{ nm}} = 0.3$. Isopropyl- β -D-thiogalactopyranoside (0.4 mM) was then added to induce the expression of GST-Tim10, and bacterial growth was continued for 3 h. The induced cell suspension was harvested, washed, and resuspended in 30 ml of lysis buffer (20 mM Tris-HCl (pH 7.4), 150 mM NaCl, 1 mM phenylmethylsulfonyl fluoride, and 10 mM β -mercaptoethanol). Cells were broken with a French press cylinder (SLM-AMINCO) at 10,000 p.s.i. and centrifuged at 21,000 $\times g$ for 30 min at 4 °C. The soluble part containing Tim10 was incubated overnight with 3 ml of glutathione-Sepharose 4B beads (Sigma) equilibrated with buffer A (50 mM Tris-HCl (pH 8.0) and 150 mM NaCl). The non-bound proteins were collected, and the beads were washed with 150 ml of buffer A. After washing, the beads were resuspended with an equal volume of buffer A, and 50 units of thrombin (Sigma) was added for overnight incubation at 4 °C. The Tim10 protein was eluted with 5 ml of buffer A.

Tim9—GST-Tim9 was produced using identical conditions of growth and induction as described for GST-Tim10. After disruption of induced cells with a French press, GST-Tim9 was found in the inclusion bodies (pellet). These were solubilized in buffer B (1 mM DTT, 150 mM NaCl, and 50 mM Tris-HCl (pH 8.0)) containing 8 M urea for 1 h at room temperature and renatured overnight at 4 °C by a 10-fold dilution with buffer B. The refolded GST-Tim9 was centrifuged at 21,000 $\times g$ for 15 min at 4 °C to eliminate remaining aggregated material, and the supernatant was incubated for 5 h with 3 ml of glutathione-Sepharose 4B beads equilibrated with buffer B. This procedure reproducibly yielded >50% renatured protein that could bind efficiently to glutathione-Sepharose beads, suggesting that at least the GST moiety was refolded to its native conformation. Further purification was done as described for Tim10, but using buffer B instead of buffer A.

Reconstitution of the TIM10 Complex—Purified Tim9 or Tim10 was concentrated up to 4–6 mg/ml using a Centrplus YM-10 membrane

(Amicon, Inc.), and then an equal amount was mixed together and incubated at 4 °C for 2 h.

Circular Dichroism Spectroscopy

CD spectra were acquired using a JASCO J810 spectropolarimeter in 5 mM Tris (pH 7.6) at 25 °C using a 1-mm cuvette and protein samples of 0.05 and 0.07 mg/ml for Tim9 and Tim10, respectively. Each spectrum represents an average of four scans from 260 to 190 nm at 0.2-nm intervals. The base line was established by subtracting the spectrum of the buffer alone.

Limited Proteolysis

Individual Tim9 or Tim10 proteins were incubated at a 1:20 (w/w) trypsin/protein ratio. Incubations were carried out at 4 °C and stopped by addition of an excess of soybean trypsin inhibitor for 10 min at 4 °C. Samples were boiled at 95 °C and analyzed by SDS-PAGE followed by Coomassie staining (see Fig. 1). To compare the individual proteins with the reconstituted complex in Fig. 3B, limited trypsinolysis was performed, but using a 1:10 trypsin/protein ratio and detection by antibodies rather than Coomassie staining to allow visualization of the proteins in the complex.

Isothermal Titration Calorimetry

Isothermal titration calorimetry for the binding of Tim9 to Tim10 was performed in 20 mM sodium phosphate (pH 7.6) at 30 °C with a VP-ITC microcalorimeter. Tim9 or Tim10 was in the 1.4-ml cuvette at 10 μ M, and 35 injections of 5 μ l of 15 \times concentrated Tim10 or Tim9 were made. Protein concentration was determined by both the Bradford assay (Bio-Rad) and amino acid analysis.

Analytical Ultracentrifugation

0.42-ml samples were centrifuged in 1.2-cm path length 2-sector aluminum centerpiece cells with sapphire windows in a 4-place An-60 Ti analytical rotor running in an Optima XL-1 analytical ultracentrifuge (Beckman Instruments) at 60,000 rpm and at a temperature of 23 °C. Changes in solute concentration were detected by Rayleigh interference. Results were analyzed using the program DCDT+ (Version 1.13) (38) by John Philo.

Chemical Cross-linking

In Tim9 experiments, samples were incubated with the homobifunctional, sulfhydryl-specific, cross-linking reagent bismaleimido-hexane (Pierce). Bismaleimido-hexane (100 or 500 μ M or 1 mM) was added to samples and incubated on ice for 30 min before being quenched by addition of 10 mM *N*-ethylmaleimide (Sigma) for a further 10-min incubation on ice. Cross-linking was performed in 50 mM Tris-HCl (pH 8.0) containing 150 mM NaCl and 1 mM DTT. After quenching, sample buffer was added to the reactions, which were boiled at 95 °C, subjected to SDS-PAGE, and then analyzed by Western blotting.

In Tim10 experiments, samples were incubated with the heterobifunctional cross-linking reagent glutaraldehyde (Sigma) (39). 500 μ M glutaraldehyde was added to samples, which were incubated on ice for 30 min. In this case, cross-linking was performed in 50 mM HEPES/KOH (pH 8.0) containing 150 mM NaCl. Reactions were quenched by addition of 100 mM Tris-HCl (pH 8.0) for 10 min on ice, after which samples were boiled with sample buffer and then analyzed by SDS-PAGE and Coomassie staining.

Light Scattering

Purified Tim10 in buffer A was chromatographed on a Superdex-75 column (Amersham Biosciences) at a flow rate of 0.2 ml/min. The effluent of the column was monitored in-line through a Dawn DSP laser photometer to measure light scattering and a Wyatt/Optilab 903 interferometric refractometer to measure sample concentration. Light scattering data were collected simultaneously at 18° between 1° and 158°, and the data were analyzed by the method of Zimm (see Refs. 40 and 41).

In Vitro Activity Assays

AAC Binding Assay—*E. coli* BL21(DE3) pLysS cells were transformed with His₆-AAC and grown on terrific broth (TB) medium supplemented with 1% glucose, 0.1 mg/ml carbenicillin, and 0.034 mg/ml chloramphenicol at 37 °C. Following removal of glucose, cells were transferred to TB medium containing 0.1 mg/ml carbenicillin and 0.034 mg/ml chloramphenicol, and His₆-AAC expression was induced by addition of 1 mM isopropyl- β -D-thiogalactopyranoside for 1 h at 37 °C. His₆-AAC was subsequently partially purified in the presence of 1%

(v/v) Triton X-100 using nickel beads (QIAGEN Inc.) according to the manufacturer's instructions. A known amount of AAC (0.5 μ g, as estimated by quantitative Western blotting using an anti-His tag antibody and a control His-tagged protein) and chymotrypsin as a control were spotted onto a nitrocellulose membrane, which was subsequently blocked for 1 h with 5% (w/v) milk in phosphate-buffered saline containing 0.1% (v/v) Tween 20. The membrane was then incubated with authentic (IMS) or recombinant TIM10 complex (1 μ g) prepared as described above plus 5% milk for 2 h. After washing, the membrane was subjected to Western blotting with anti-Tim9 or anti-Tim10 antibodies. Control incubations of buffer alone or the TIM10 complex denatured by heating at 95 °C for 5 min with 10 mM DTT and 10 mM EDTA were also carried out prior to Western blotting. Chemiluminescence data were collected using a Fuji LAS-1000 luminescent image analyzer. Each spot on the Western blot was subjected to densitometry using the AIDA Version 2.31 software supplied with the analyzer, and a histogram was produced from data acquired from three independent identical experiments.

Luciferase Refolding Assay—Luciferase (Sigma) was stored at 328 μ M in enzyme buffer consisting of 50 mM HEPES (pH 7.4) and 150 mM NaCl and was denatured at 5.0 μ M for 30 min at 25 °C in 30 mM HEPES (pH 7.4) containing 6 M guanidine HCl and 5 mM DTT. The denatured enzyme was typically diluted 1:125 to 40 nM in refolding buffer consisting of 10 mM MOPS/KOH (pH 7.2) and 50 mM KCl in the presence of the Tim proteins or the complex at the same monomer concentration (15 \times molar excess over luciferase). The positive control used in the assay was the DnaK/DnaJ/GrpE chaperone system (Stressgen Biotech Corp.) at 80/400/400 nM, respectively (2:10:10 ratio over luciferase). DnaJ was incubated for 15 min in refolding buffer prior to addition of luciferase. Upon addition of the enzyme, the reaction mixture was incubated for 5 min at 25 °C; DnaK was then added; and refolding was initiated by addition of GrpE after a further 5-min incubation. The negative control consisted of denatured luciferase in refolding buffer, with the total assay volume being 200 μ l. All components in this assay were compared with native enzyme at the same concentration. Native enzyme was stored at 4 °C at a concentration of 5 μ M in enzyme buffer and then diluted 1:125 in refolding buffer at 25 °C to give a total volume of 200 μ l. Aliquots of 4 μ l were then removed at the desired time intervals and added to a luciferase assay detection kit (Promega), consisting of 50 μ l of luciferase assay reagent and 10 μ l of cell lysis buffer (containing 6 mg/ml BSA) in a 96-well plate. The plate was then read in a PerkinElmer Life Sciences LB96P luminometer for 10 s.

Miscellaneous Methods

Blue native gel electrophoresis, Western blotting, gel filtration, and immunoprecipitations were performed as described previously (31).

RESULTS

Purification and Folding of Tim10 and Tim9—Tim10 was expressed as a GST fusion protein at high levels (see "Experimental Procedures") and remained largely soluble. After binding to the glutathione-Sepharose beads and cleavage by thrombin, a single band of \sim 10 kDa was detected by Coomassie staining (Fig. 1A). The identity of this band was verified by Western blotting with anti-Tim10 antibodies (data not shown) and N-terminal sequencing, which confirmed the N terminus to be Gly-Ser-Met-Ser (Gly and Ser are two residues resulting from the cloning into the *Bam*HI site of the pGEX vector, and Met and Ser are the first two residues of Tim10). This suggested that thrombin cleavage was indeed specific, resulting in a chemically homogeneous Tim10 preparation. Secondary structure prediction for the Tim10 sequence (performed with the PHDsec (42) and DSC (43) programs) predicted a 55–60% α -helical structure for the protein and very little β -sheet content. To test whether the purified Tim10 protein was folded and to examine its secondary structure, far-UV circular dichroism was performed. Spectra of native Tim10 were compared with those of the protein denatured by guanidine HCl (Fig. 1B). This spectrum of pure Tim10 displays two minima at 209 and 222 nm, which are typical for α -helical structure. In an alternative approach to test whether the protein was folded, we performed limited trypsinolysis (Fig. 2C). At a 1:20 (w/w) trypsin/protein ratio, a stable fragment of \sim 7 kDa remained intact even after

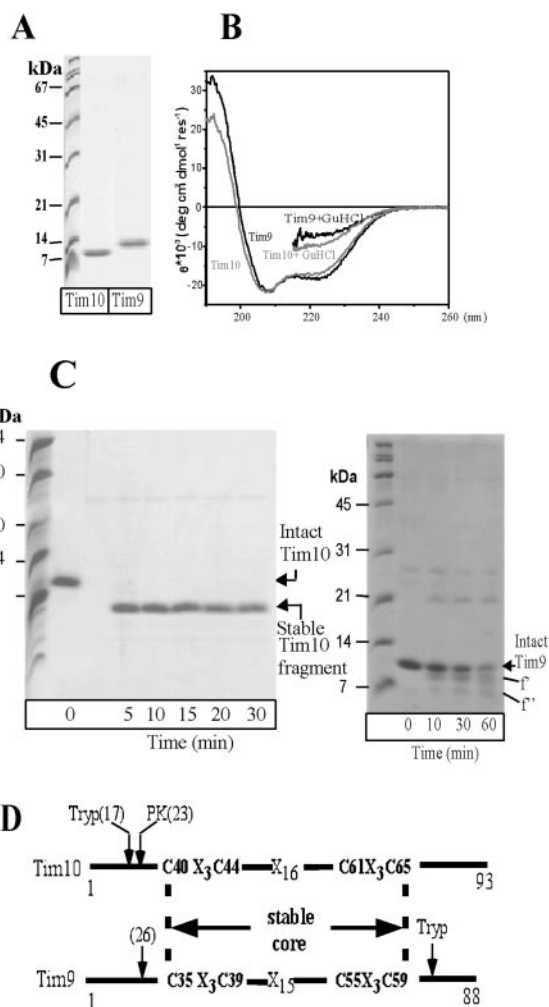


FIG. 1. Purification and characterization of Tim9 and Tim10. A, purification of Tim9 and Tim10. Recombinant GST-Tim9 was purified from inclusion bodies, and recombinant GST-Tim10 was purified from the supernatant using glutathione-Sepharose beads (see "Experimental Procedures"). The purifications were followed by SDS-PAGE and Coomassie Blue staining. B, circular dichroism of Tim9 and Tim10. The far-UV CD spectra of Tim9 and Tim10 in either buffer or 6 M guanidine HCl (*GuHCl*) are shown. The signals were divided by the total number of residues of 87 for Tim9 and 93 for Tim10. Each spectrum is an average of four scans. C, limited proteolysis of Tim9 or Tim10 with trypsin. Reactions were carried out at 4 °C for the indicated times and stopped by addition of soybean trypsin inhibitor. Samples were boiled at 95 °C and analyzed by SDS-PAGE followed by Coomassie staining. Intact and stable fragments are indicated by arrows. *f'* and *f''* indicate Tim9 stable fragments (see "Results" for details). D, schematic diagram of the sequences of Tim9 and Tim10. The positions of protease cleavage (*Tryp*, trypsin; *PK*, proteinase K or spontaneous cleavage) are shown in parentheses (see "Results" for details). The stable, protease-resistant core is delineated by a dashed line.

30 min of trypsinolysis ("stable Tim10 fragment") (Fig. 1C). The N-terminal sequence of this fragment (Ile-Gln-Ala-Ala) starts at position 18 in the sequence of Tim10. A similar N-terminal truncated fragment was obtained with proteinase K (starting at position 24, with the N-terminal sequence determined as Ala-Glu-Leu-Asp), but was further degraded with longer incubation times (data not shown). A similarly sized stable fragment was spontaneously obtained upon long incubations (more than a few weeks) of the intact Tim10 protein at 4 °C. This shows that Tim10 has a protease-resistant core of \sim 7 kDa and a flexible N-terminal tail.

Unlike Tim10, GST-Tim9 was intrinsically insoluble, and up to 75% of the protein accumulated in inclusion bodies (31). This

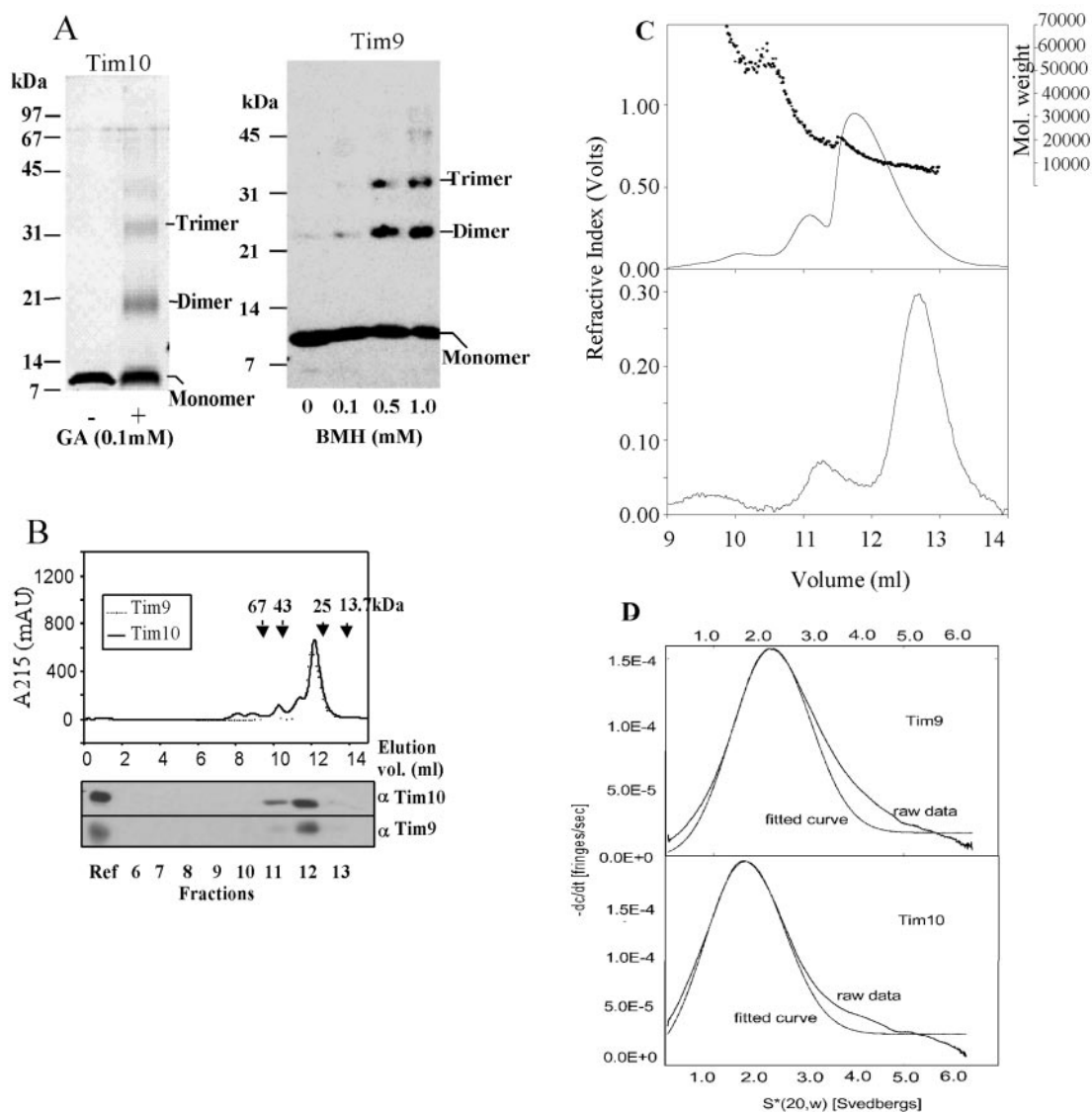


FIG. 2. Pure Tim9 and Tim10 self-associate to form oligomers. *A*, cross-linking of Tim9 or Tim10. Purified Tim10 was incubated on ice for 30 min without (–) or with (+) glutaraldehyde (GA). Reactions were quenched by addition of 100 mM Tris-HCl (pH 8.0) and analyzed by SDS-PAGE followed by Coomassie blue staining. Purified Tim9 was incubated on ice for 30 min with the cross-linker bismaleimido-hexane (BMH). Reactions were quenched by addition of an excess of *N*-ethylmaleimide and analyzed by SDS-PAGE followed by Western blotting using rabbit anti-Tim9 polyclonal antibodies. *B*, gel filtration of individual Tim9 or Tim10. 500 μ g of purified Tim9 or Tim10 was loaded onto a Superdex-75 column at a flow rate of 0.5 ml/min. 1-ml fractions were collected and analyzed by SDS-PAGE followed by immunoblotting using rabbit anti-Tim9 or anti-Tim10 polyclonal antibodies. The molecular mass standards for the Superdex-75 gel filtration column were ribonuclease A (13.7 kDa), chymotrypsinogen A (25 kDa), ovalbumin (43 kDa), and BSA (67 kDa). *mAU*, milli-absorbance units; *Ref*, reference. *C*, light scattering of Tim10. Multi-angle light scattering analysis (see “Experimental Procedures”) of Tim10 was performed on the effluent from a Superdex-75 column eluting at 0.2 ml/min. Samples containing different quantities of Tim10 in 500 μ l of buffer were injected onto the column. The data are shown for 500 μ g (upper panel) and 5 μ g (lower panel). Recovery of the protein was >90%. The refractive index data are on the left *y* axis (solid line), and the molecular mass data are on the right *y* axis (dotted line). *D*, analytical ultracentrifugation of Tim9 or Tim10. The sedimentation coefficients for Tim9 and Tim10 are plotted with respect to the time derivative of the concentration profile. $s_{20,w}$ values of 2.05 for Tim9 and 1.51 for Tim10 were found.

is in agreement with the behavior of the protein *in vivo*: in mitochondria lacking Tim10, Tim9 does not stay soluble in the intermembrane space and sediments with the membrane fraction in mitoplasts. To purify Tim9 from *E. coli*, we therefore isolated GST-Tim9 from inclusion bodies (see “Experimental Procedures”). Upon cleavage of GST-Tim9 with thrombin, a single band of the expected size was isolated (Fig. 1A, last lane). This band could be recognized by monospecific anti-Tim9 antibodies (data not shown). N-terminal sequencing confirmed that the protein was intact and that there were no spurious cleavage products from thrombin. Upon extended incubation at 4 °C, Tim9 was degraded to give a stable fragment of ~6 kDa. N-terminal sequencing of this fragment showed its N terminus

to be Leu²⁷ in the sequence of Tim9, suggesting that, as for Tim10, the N terminus of Tim9 is flexible with a stable core delineated by the “twin CX₃C” motif (Fig. 1D). A related degradation pattern was observed in limited proteolysis experiments as shown in Fig. 1C (right panel). Although Tim9 appeared to be more stable than Tim10 against trypsin, two Tim9 stable fragments were observed, ~1 and 3 kDa shorter than the intact protein. N-terminal sequencing of the 1-kDa deleted form (*f'*) was not successful, presumably because the protein was blocked. However, N-terminal sequencing of the second fragment (*f''*) revealed two species: a major one of the same N-terminal sequence (Gly-Ser-Met-Asp-Ala-Leu) as the full-length protein, indicating that this results from a truncation of

its C terminus, and a minor one truncated at the N terminus. The central part of Tim9 between the two CX₃C motifs hence comprises a stable domain. CD spectroscopy showed that pure Tim9 had very similar molar ellipticity compared with Tim10, characteristic of α -helices (Fig. 1B). Taken together, these data suggest that both individual proteins are mainly α -helical and contain a protease-resistant central core comprising the twin CX₃C motif.

Tim10 and Tim9 Form Homo-oligomers—What is the native size of pure Tim10 and Tim9? The state of the individual proteins is relevant to the physiological situation *in vivo*, as it reflects the state of the two proteins in the cytosol, where they are unassembled. Complex formation presumably occurs only after import into mitochondria. We first performed chemical cross-linking with either glutaraldehyde (cross-linking mainly lysine residues) (Fig. 2A, *left panel*) or bismaleimido-hexane (a homobifunctional, cysteine-specific cross-linker) (*right panel*). Both proteins have the ability to form mainly homodimers, but also, to a lesser extent, trimers and higher oligomers (Fig. 2A). The yield of homo-oligomeric cross-links was dependent on the concentration of the cross-linker (Fig. 2A, *right panel*). Similar results were obtained using another homobifunctional, lysine-specific cross-linker, bis(sulfosuccinimidyl) suberate (length of 11.4 Å) (data not shown).

However, the observed homo-oligomeric species could be only transient and/or only induced by chemical cross-linking. To test whether the homo-oligomeric forms represent native species, we performed gel filtration analysis (Fig. 2B). Both Tim10 and Tim9 migrated mainly in fraction 12, which corresponds to ~25 kDa and would therefore be a dimer based on the molecular mass calibration of the column. Trimeric species were also observed (fraction 11), albeit at much lower intensities, in agreement with the chemical cross-linking data. We further investigated these findings by performing gel filtration analysis with in-line multi-angle light scattering (40, 41) to determine directly the molecular mass distribution across the chromatographic profile. The data clearly indicate that the major peak (measured to account for 78% weight fraction of the total) is a reaction boundary between dimeric and monomeric species (Fig. 2C). Dilution of the sample moved the equilibrium toward the monomeric species, as shown by the increased elution volume and the more gaussian appearance of the main peak (Fig. 2C, *lower panel*). Interestingly, there were also significant amounts of trimeric (14% weight fraction) and hexameric (7% weight fraction) species at high concentrations (Fig. 2C, *upper panel*), but also at low concentrations (*lower panel*). It would appear that these higher multimers are not necessarily part of the monomer-dimer association process, but may constitute a distinct subfraction present in a different state (see “Discussion”).

The cross-linking, gel filtration, and light scattering data taken together suggest that the Tim9 and Tim10 proteins dynamically self-associate to form oligomers. The apparent molecular mass of the major fraction of Tim9 and Tim10 homo-oligomers would be consistent with either elongated dimers or very compacted trimers. To distinguish between these alternatives, we used sedimentation equilibrium, as this provides a molecular mass estimate that is independent of shape (Fig. 2D). From sedimentation equilibrium analysis, the apparent mass was calculated with respect to concentration (at a range of concentrations between 0.1 and 0.4 mg/ml) and found to be a maximum of 20 kDa for either Tim9 or Tim10. The sedimentation equilibrium data hence also suggest that the two proteins are mostly dimeric. Sedimentation velocity was then performed under similar conditions to characterize their hydrodynamic behavior. Tim10 was found to sediment with a

sedimentation coefficient ($s_{20,w}$) of 1.51, whereas Tim9 had an $s_{20,w}$ of 2.05 (Fig. 2D), suggesting that Tim9 is more extended than Tim10.

Tim9 and Tim10 Stabilize Each Other and Assemble into the TIM10 Complex with Submicromolar Affinity—Tim9 and Tim10 form a complex when coexpressed from a single plasmid in *E. coli* (31, 37). Under these conditions, the two proteins can interact during their synthesis in possibly a partially folded state. Here, we wanted to address whether the two proteins can interact to form a functional complex after completion of their synthesis and after having been separately purified. This situation is more relevant to the *in vivo* conditions, as both Tim9 and Tim10 are presumably fully synthesized in the cytosol and then imported post-translationally into mitochondria, where assembly of the TIM10 complex occurs.

A first indication that the two separately purified proteins can indeed interact came from the observation that *E. coli* cell-expressed GST-Tim9 (which is intrinsically less soluble and has to be denatured in urea and then renatured) was rendered more soluble by Tim10 when the two proteins were concentrated together. Essentially all of Tim9 remained soluble during concentration when incubated with Tim10 (Fig. 3A, compare *third* and *fourth lanes*). This was a specific effect of the Tim10 protein, as BSA used as a control did not have any effect (Fig. 3A, *fifth lane*).

Stabilization of the two proteins when incubated together was further examined by limited proteolysis with trypsin using both the TIM10 complex as well as the individual proteins (Fig. 3B). The trypsin/protein mass ratio in this case was 1:10, and antibody detection was used. Both proteins were protected against proteolysis in their assembled form (Fig. 3B, *right panel*) as opposed to when they were alone (*left panel*), suggesting either the formation of more stable structures or protection of cleavage sites through steric hindrance following complex formation.

To demonstrate direct interaction, we incubated Tim10 and Tim9 together and analyzed the resulting mixture by gel filtration chromatography. Fractions were then analyzed by SDS-PAGE and immunodetection. Using this method, we observed the disappearance of the peaks seen with the individual proteins (25 kDa) and the appearance of a new peak with an apparent molecular mass of 50–60 kDa (fractions 9 and 10) (Fig. 3C), indicating complex formation. This molecular mass is similar to that of the mitochondrial TIM10 complex (Fig. 3C, *Native TIM10*). The remaining peaks in fractions 11 and 12 most likely correspond to unassembled molecules. To exclude the possibility that the two proteins are in two separate homo-oligomeric complexes simply coeluting, we performed co-immunoprecipitations from fraction 9 (Fig. 3D). Both Tim9 and Tim10 could be co-immunoprecipitated with antibodies against the other, which strongly suggests the formation of an authentic TIM10 complex. As a third method to show complex formation, we used blue native gel electrophoresis, which also indicated formation of a TIM10 complex at ~60–70 kDa, similar to the intermembrane space complex (Fig. 3E). The slight difference in size of the TIM10 complex upon blue native gel electrophoresis could be due to the use of detergent in the buffers, in contrast to gel filtration analysis, which is performed in detergent-free buffers.

We further characterized the hydrodynamic properties of the complex by sedimentation velocity. We found a sedimentation coefficient ($s_{20,w}$) of 4.05, which is similar to the sedimentation coefficient of 4.07 for the 68-kDa monomeric fragment of SecA (44). However, the frictional coefficient ratio (f/f_0) was found equal to 1.95, which indicates that the TIM10 complex is a significantly extended particle (for comparison, BSA with a

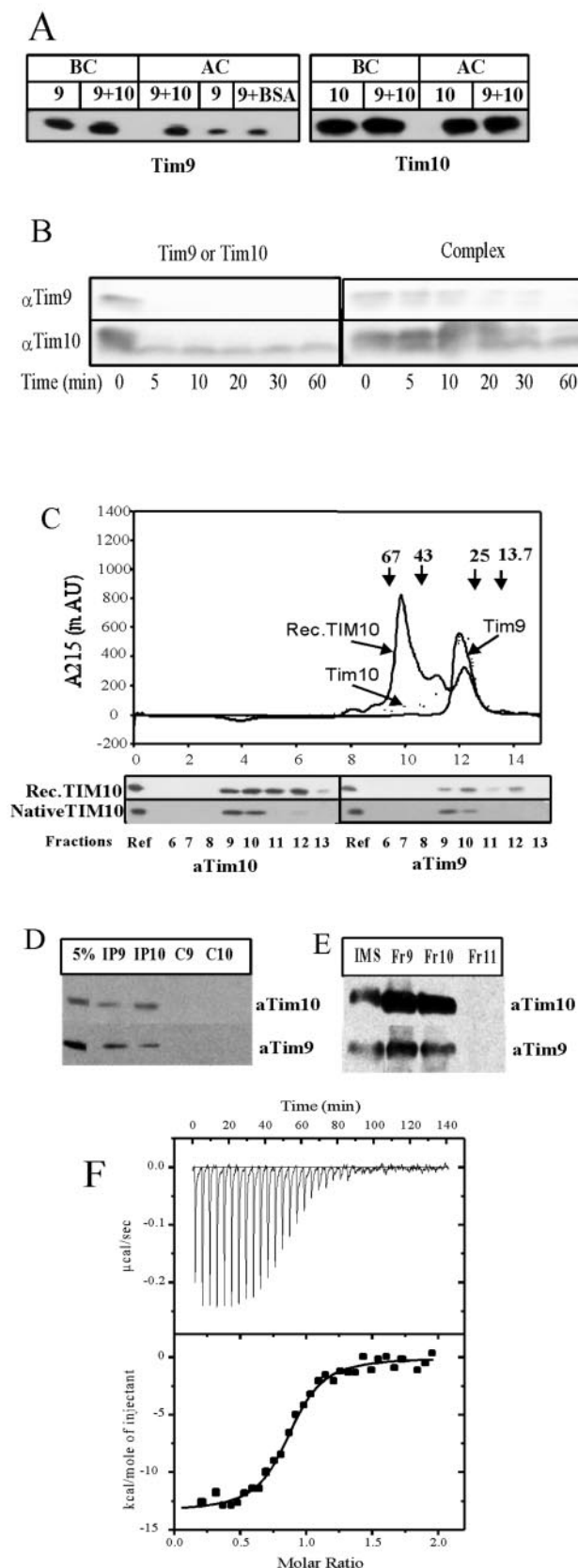


FIG. 3. Tim9 and Tim10 assemble to form the TIM10 complex. *A*, Tim10 stabilizes Tim9. Solutions containing Tim9 (9), Tim10 (10), Tim9 and Tim10 together (9+10), or Tim9 and BSA (9+BSA) were concentrated 13-fold (starting concentration in each protein of 0.02 mg/ml, 10 μ g of each protein or BSA) in Microcon YM-3 microconcentrators and then centrifuged to remove insoluble proteins. These supernatants were analyzed by SDS-PAGE and Western blotting with antibodies against Tim9 and Tim10 as indicated. *BC*, before concentration;

molecular mass of 65 kDa and hemoglobin with a molecular mass of 68 kDa have frictional coefficient ratios of 1.33 and 1.28, respectively).

Having the two proteins in a chemically pure state and able to form a complex, it was important to characterize the thermodynamic properties of their interaction (stoichiometry and affinity). We carried out isothermal titration calorimetry at 30 $^{\circ}$ C, which is the physiological temperature for yeast proteins and hence for this interaction to occur (Fig. 3*F*). We determined the stoichiometry to be 1:1, which is in agreement with our own semiquantitative measurements using antibodies (25)² or using radiolabeled mitochondria (26). Tim10 bound to Tim9 with a high, physiologically significant affinity ($K_a = 0.5 \mu\text{M}$ or $K_d = 0.2 \mu\text{M}$), which explains the stability of the complex once formed. The same result was obtained when Tim10 was placed in the cuvette and Tim9 was injected (data not shown).

Activity of the TIM10 Complex in a Mitochondrion-free Assay—TIM10 mediates transport of hydrophobic proteins like AAC across the aqueous intermembrane space until they insert at the inner membrane. It is generally thought that, in this process, the TIM10 complex functions as a chaperone (2, 31, 37, 45). Here, we wanted to address the interaction of TIM10 with its physiological substrate AAC (Fig. 4*A*).

Reconstituted TIM10 was incubated with membrane-immobilized purified yeast AAC1, followed by anti-Tim9 and anti-Tim10 immunodetection. We found that the TIM10 complex bound to AAC (Fig. 4*A*, bar 3), but not to inactivated chymotrypsin (bar 4), an unrelated control protein. The levels of pure TIM10 complex binding were comparable to those obtained using the native IMS fraction (Fig. 4*A*, bar 2), containing equivalent amounts of TIM10 (based on quantitative immunoblotting). The denatured complex (treated with DTT/EDTA and heated at 95 $^{\circ}$ C) showed a much reduced binding (Fig. 4*A*, bar 5). This overlay binding assay constitutes the first report of direct binding of the TIM10 complex to full-length AAC in a mitochondrion-free environment and shows there is an intrinsic affinity of the TIM10 complex for AAC.

To further test the activity of TIM10 as a chaperone, we monitored refolding of denatured firefly luciferase, a model

² S. Vial and K. Tokatlidis, unpublished data.

AC, after concentration. *B*, limited proteolysis of the TIM10 complex compared with the individual Tim9 and Tim10 proteins. Reactions were carried out at 4 $^{\circ}$ C and analyzed by SDS-PAGE and Western blotting. *C*, gel filtration analysis of Tim9 and Tim10 incubated together. The recombinant TIM10 complex curve (*Rec. TIM10*) is represented with a thick line. Eluted fractions were analyzed by SDS-PAGE and Western blotting using anti-Tim9 (*aTim9*) or anti-Tim10 (*aTim10*) polyclonal antibodies. The Tim9 (*thin line*) and Tim10 (*dotted line*) chromatography traces were overlaid on the same graph as a reference. *Native TIM10* refers to the IMS complex analyzed under the same conditions. *mAU*, milli-absorbance units; *Ref*, reference. *D*, co-immunoprecipitation of Tim9 and Tim10. 20 μ l of fraction 9 collected from the gel filtration of the Tim9 and Tim10 mixture was subjected to immunoprecipitation using anti-Tim9 (*IP9*), anti-Tim10 (*IP10*), preimmune Tim9 (*C9*), or preimmune Tim10 (*C10*) antisera. Each immunoprecipitation was analyzed by SDS-PAGE and Western blotting using antibodies against Tim9 and Tim10. The 5% control corresponds to 5% of the starting immunoprecipitated material. *E*, blue native PAGE. 1 μ g of IMS (*first lane*) and 20 μ l of fractions 9 (*Fr9*; *second lane*), 10 (*Fr10*; *third lane*), and 11 (*Fr11*; *fourth lane*) from the Superdex-75 gel filtration column were subjected to blue native gel electrophoresis, blotted onto a nitrocellulose membrane, and immunodecorated using antibodies against Tim9 or Tim10. *F*, isothermal titration calorimetry. *Upper panel*, trace of the titration of 35 injections of 5 μ l each of 150 μM Tim10 into 10 μM Tim9 measured by a VP-ITC microcalorimeter; *lower panel*, the integrated and normalized heats of injections for the binding (*filled squares*). Data were fitted to a model describing one binding site (*solid line*). Analysis of the data yielded a Tim9/Tim10 stoichiometry of 0.9, $K_a = 5 \times 10^6 \text{ M}^{-1}$ (or $K_d = 0.2 \mu\text{M}$), and $\Delta H = -13 \text{ kcal/mol}$.

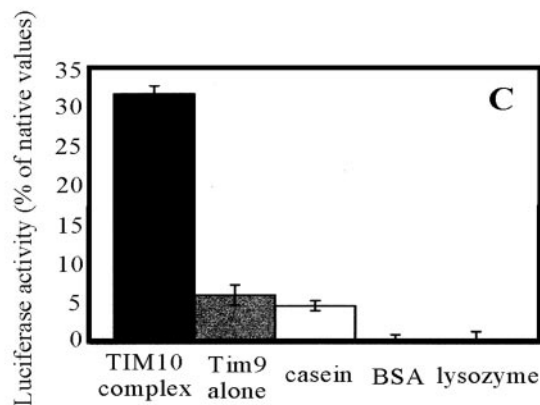
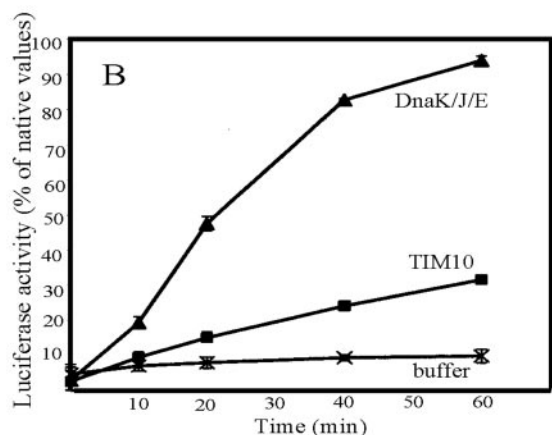
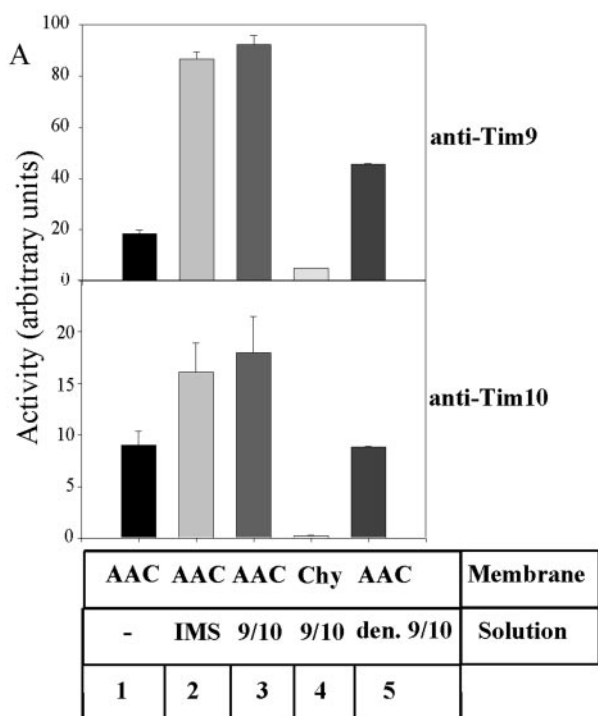


FIG. 4. Reconstituted TIM10 complex is active under mitochondrion-free conditions. *A*, binding of the TIM10 complex to full-length AAC *in vitro*. Nitrocellulose membranes were spotted with either AAC or chymotrypsin (*Chy*) as indicated and overlaid with IMS, the reconstituted TIM10 complex (9/10 (native) or *den.* (denatured) 9/10), or buffer only (-). After washing, the membranes were subjected to Western blotting using antibodies against Tim9 (*upper panel*) or Tim10 (*lower panel*). The spots obtained were subsequently analyzed by densitometry, and a histogram was generated from three independent

substrate (46), in the presence or absence of TIM10 and compared it with the activity of the DnaK/DnaJ/GrpE system, a well studied cytosolic chaperone (47, 48). The DnaK/DnaJ/GrpE system was chosen because it has been used extensively in luciferase refolding assays, and DnaJ has a zinc-binding motif that was shown to bind to the denatured substrate (49). In this assay, DnaK/DnaJ/GrpE yielded >90% active enzyme (Fig. 4*B*). Incubation with buffer gave only background activity. However, incubation with the recombinant TIM10 complex showed a significant increase in luciferase activity with a shape similar to that of the DnaK/DnaJ/GrpE system, but with a weaker final yield after 60 min (30–40%) (Fig. 4, *B* and *C*, *first bar*). Two control proteins, BSA and lysozyme, did not show any activity at all, whereas casein, a strongly hydrophobic protein, showed some weak activity (Fig. 4*C*). The effect of casein leveled off after ~30 min of incubation, in contrast to that of DnaJ or TIM10 complex activity, which increased with time. Tim9 and Tim10 on their own, even when used in excess or simply mixed in an unassembled form, showed only residual activity, and their effect leveled off in the same way as casein (data not shown), indicating this corresponds to background activity, possibly due to hydrophobic interactions (Fig. 4*C*, *second bar*). These results suggest that the fully assembled TIM10 complex has measurable chaperone activity *in vitro*.

DISCUSSION

In this work, we have purified and structurally characterized the individual Tim9 and Tim10 proteins and have reconstituted them in a functional TIM10 complex. We have measured the affinity and subunit stoichiometry underlying this assembly process and have developed a mitochondrion-free activity assay for the pure complex against (i) a physiological substrate (AAC) and (ii) a non-mitochondrial enzyme (luciferase).

Both Tim9 and Tim10 appear to be folded in α -helical conformation. A novel feature revealed here is that both proteins contain a flexible N terminus (~25% of the total sequence) and, in the case of Tim9, apparently a flexible C terminus as well. More importantly, they both have a more stable central domain. This raises the possibility that these distinct structural motifs might also have distinct functions. Experiments are under way in our laboratory to address this point. The stable core comprises the whole of the predicted zinc finger-like motif (29); although recently, Curran *et al.* (37) reported that the TIM10 complex does not bind zinc, and the proteins were in an oxidized state in our experiments.

Tim10 renders Tim9 soluble by preventing its aggregation and by stabilizing it upon complex formation. Does this interaction have any relevance *in vivo*? It could be that Tim10 is imported first into mitochondria and then functions as a scaffold for Tim9, upon which Tim9 binds to form a stable TIM10 complex. In this model, one would expect that a Tim10 homooligomer should be thermodynamically stable on its own. We indeed observed that Tim10 exists as an independent protein that self-associates to form mainly dimers/trimers in solution.

Can the individually purified proteins form a complex? In a previous report, we had shown that, upon coexpression of the subunits, an authentic TIM10 complex could be formed, indistinguishable from the IMS complex (31). Recently, Curran *et al.*

experiments. *B*, TIM10 chaperones denature luciferase in an *in vitro* refolding assay. Luciferase was denatured at 5 μ M and diluted 1:125 in refolding buffer in the presence of the indicated constituents as described under "Experimental Procedures." The values for luciferase activity are percentages of the native enzyme values. *C*, recovery of luciferase activity (percentage of the native values) after 60 min of refolding using the indicated proteins at the same concentration. Casein, lysozyme, and BSA were included as controls.

(37) confirmed our data, adopting a similar coexpression strategy. In both studies, the two proteins could interact while being synthesized or with the transient help of an *E. coli* chaperone not present in the final reconstituted complex. To exclude these possibilities, we tested whether TIM10 can be formed from its subunits after these are individually purified. This situation is more physiologically relevant, as the two proteins have to be imported first as full-length polypeptides and then interact in the IMS. The assembly of TIM10 reported here was tested by four different methods: gel filtration, blue native gel electrophoresis, co-immunoprecipitation, and isothermal titration calorimetry. Isothermal titration calorimetry was used to measure for the first time the affinity of this binding event, which was found to be in the submicromolar range. This is a significantly high affinity and physiologically relevant and would explain the stability of the complex when we purified it from mitochondria, where it can resist three separate chromatography steps (25). It also corroborates our previous finding that no other mitochondrial protein is necessary to form the TIM10 complex. It would also indicate that the substrate AAC is not necessary for assembling Tim9 and Tim10 and that it presumably binds to a stable, preformed complex. We have also precisely measured the stoichiometry of the complex, which was found to be 1:1, in agreement with our semiquantitative method using mitochondrial extracts and immunoblotting (25)² or use of radioactively labeled mitochondria (26). This stoichiometry and our sedimentation analysis now provide strong evidence that the TIM10 complex consists of three molecules of Tim9 and three molecules of Tim10.

How does the heterohexameric TIM10 complex assemble from its subunits? The individual proteins are mainly dimeric, but they can also exist in a trimeric state (as this was directly demonstrated in the Tim10 light scattering experiments (Fig. 2C)), which might be favored at higher concentrations or in the presence of the partner subunit. Assembly between dynamic homo-oligomers would result in formation of a stable slower dissociating heterohexamer. In this model, the assembly process would involve significant structural rearrangements of the constituting subunits. Our experiments with the individual proteins that show dynamic self-association and dissociation (gel filtration and light scattering experiments) support this working model. Experiments using structural techniques able to distinguish among dynamic conformational changes are needed to test this working model.

Once the complex is formed, it is thermodynamically very stable, as indicated by the high binding constant. What is the implication of this for its role *in vivo*? This would argue in favor of a mechanism where the TIM10 complex transfers only AAC onto the downstream 300-kDa complex without dissociating upon transfer to its subunits and without any dynamic redistribution of the small Tim proteins (namely Tim12) from the 300-kDa complex into the 70-kDa complex. In agreement with this, we found that pure Tim12 cannot dissociate the TIM10 complex *in vitro* when incubated together.³ Our working hypothesis for the role of the 70-kDa TIM10 complex in this mechanism is that (i) it functions purely as a chaperone protecting AAC from aggregation; (ii) it remains stable as a heterohexamer; and (iii) passage of AAC onto the TIM22 complex for proper insertion is mediated by direct binding of AAC to the TIM22 complex accompanied by allosteric release of AAC from the TIM10 complex.

All the reconstitution studies of the TIM10 complex to date have been hampered by the lack of a reliable *in vitro* binding system. Here, we have presented two assays in which the pure

TIM10 complex showed activity under completely mitochondrion-free conditions. First, we showed that the TIM10 complex could bind to AAC in an overlay assay in which full-length AAC had been immobilized onto a membrane. Previous work showed significant *in vitro* interaction between purified cytosolic receptor domains and preproteins (5–7, 50, 51). More recently, cellulose-immobilized peptide scans were used to delineate binding sequences of receptors against presequence-containing or presequence-devoid mitochondrial proteins (8). Finally, Curran *et al.* (37) adopted this method to show an interaction of AAC peptides with the TIM10 complex. This was done under immobilization conditions similar to those in our overlay assay, with the difference that they used peptide fragments and not the whole protein. Establishing an assay between the full-length hydrophobic carrier proteins and TIM10 has been very difficult until now. Here, we report binding of the TIM10 complex to full-length AAC, which is important, as multiple internal targeting signals distributed throughout the whole sequence are necessary for efficient translocation (8, 21, 36, 52, 53). We hypothesize that this assay works because the protein is at least partially unfolded on the membrane, thereby exposing determinants that could bind to the TIM10 complex. These regions are most likely buried when AAC is analyzed in solution, where the presence of a detergent is required to prevent its aggregation (54).

We have also shown in a separate assay that TIM10 has a measurable chaperone activity in facilitating refolding of denatured luciferase, a model substrate. This is a significant new composite feature for the TIM10 complex, in agreement with its proposed function *in vivo* (2, 31, 37, 45). Importantly, the chaperone function was observed only for the fully assembled TIM10 complex at significant levels, well above those of the individual subunits, which showed only background activity (Fig. 4C). This chaperone activity of TIM10 is weaker than that of the DnaK/DnaJ/GrpE system, which we used as a comparison. DnaJ was chosen as it contains two zinc-binding motifs, and they have been reported to mediate its chaperone function (49). The hypothetical zinc finger-like motif of Tim9 and Tim10 could also be involved in the chaperone function of the complex in a similar manner. One major difference that could explain the weaker chaperone activity of TIM10 is that the DnaJ system is powered by ATP hydrolysis and a cycle involving DnaK and GrpE, making it a very efficient system. In contrast, TIM10 does not contain any ATP-powered component, and the energy for interactions involved in carrying out its function would come from conformational changes.

Acknowledgments—We thank members of our laboratory and Drs. Colin Stirling, Stephen High, Philip Woodman, and Tassos Economou for discussions and comments on the manuscript; Dr. Sabrina Dyall for help with His₆-AAC purification; Dr. Pierre Luciano for characterization of the anti-Tim10 antibodies; Dr. Philip Woodman for use of a plate reader; Andy Baron (University of Leeds) for the analytical ultracentrifugation; Peter Sharratt (University of Cambridge) for amino acid analysis; Dr. Jean Gagnon (Institut de Biologie Structurale-Grenoble) for peptide sequencing; and Drs. Kaye Truscott and Nikolaus Pfanner for communicating unpublished results.

REFERENCES

- Schatz, G., and Dobberstein, B. (1996) *Science* **271**, 1519–1526
- Pfanner, N., and Geissler, A. (2001) *Nat. Rev. Mol. Cell. Biol.* **2**, 339–349
- Neupert, W. (1997) *Annu. Rev. Biochem.* **66**, 863–917
- Ryan, K. R., and Jensen, R. E. (1995) *Cell* **83**, 517–519
- Komiya, T., Rospert, S., Schatz, G., and Mihara, K. (1997) *EMBO J.* **16**, 4267–4275
- Komiya, T., Rospert, S., Koehler, C., Looser, R., Schatz, G., and Mihara, K. (1998) *EMBO J.* **17**, 3886–3898
- Brix, J., Dietmeier, K., and Pfanner, N. (1997) *J. Biol. Chem.* **272**, 20730–20735
- Brix, J., Rudiger, S., Bukau, B., Schneider-Mergener, J., and Pfanner, N. (1999) *J. Biol. Chem.* **274**, 16522–16530
- Schatz, G. (1997) *Nature* **388**, 121–122
- Abe, Y., Shodai, T., Muto, T., Mihara, K., Torii, H., Nishikawa, S., Endo, T.,

³ P. Savory and K. Tokatlidis, unpublished data.

- and Kohda, D. (2000) *Cell* **100**, 551–560
11. Muto, T., Obita, T., Abe, Y., Shodai, T., Endo, T., and Kohda, D. (2001) *J. Mol. Biol.* **306**, 137–143
 12. Hill, K., Model, K., Ryan, M. T., Dietmeier, K., Martin, F., Wagner, R., and Pfanner, N. (1998) *Nature* **395**, 516–521
 13. Rapaport, D., Kunkele, K. P., Dembowski, M., Ahting, U., Nargang, F. E., Neupert, W., and Lill, R. (1998) *Mol. Cell Biol.* **18**, 5256–5262
 14. Model, K., Meisinger, C., Prinz, T., Wiedemann, N., Truscott, K. N., Pfanner, N., and Ryan, M. T. (2001) *Nat. Struct. Biol.* **8**, 361–370
 15. Model, K., Prinz, T., Ruiz, T., Radermacher, M., Krimmer, T., Kuhlbrandt, W., Pfanner, N., and Meisinger, C. (2002) *J. Mol. Biol.* **316**, 657–666
 16. Kunkele, K. P., Heins, S., Dembowski, M., Nargang, F. E., Benz, R., Thieffry, M., Walz, J., Lill, R., Nussberger, S., and Neupert, W. (1998) *Cell* **93**, 1009–1019
 17. Truscott, K. N., Kovermann, P., Geissler, A., Merlin, A., Meijer, M., Driessen, A. J., Rassow, J., Pfanner, N., and Wagner, R. (2001) *Nat. Struct. Biol.* **8**, 1074–1082
 18. Lohret, T. A., Jensen, R. E., and Kinnally, K. W. (1997) *J. Cell Biol.* **137**, 377–386
 19. Taylor, A. B., Smith, B. S., Kitada, S., Kojima, K., Miyaura, H., Otwinowski, Z., Ito, A., and Deisenhofer, J. (2001) *Structure* **9**, 615–625
 20. Adrian, G. S., McCammon, M. T., Montgomery, D. L., and Douglas, M. G. (1986) *Mol. Cell Biol.* **6**, 626–634
 21. Pfanner, N., Hoeben, P., Tropfshchug, M., and Neupert, W. (1987) *J. Biol. Chem.* **262**, 14851–14854
 22. Pfanner, N., and Neupert, W. (1987) *J. Biol. Chem.* **262**, 7528–7536
 23. Sirrenberg, C., Endres, M., Folsch, H., Stuart, R. A., Neupert, W., and Brunner, M. (1998) *Nature* **391**, 912–915
 24. Koehler, C. M., Jarosch, E., Tokatlidis, K., Schmid, K., Schweyen, R. J., and Schatz, G. (1998) *Science* **279**, 369–373
 25. Koehler, C. M., Merchant, S., Oppliger, W., Schmid, K., Jarosch, E., Dolfini, L., Junne, T., Schatz, G., and Tokatlidis, K. (1998) *EMBO J.* **17**, 6477–6486
 26. Adam, A., Endres, M., Sirrenberg, C., Lottspeich, F., Neupert, W., and Brunner, M. (1999) *EMBO J.* **18**, 313–319
 27. Ryan, M. T., Muller, H., and Pfanner, N. (1999) *J. Biol. Chem.* **274**, 20619–20627
 28. Wachter, C., Schatz, G., and Glick, B. S. (1992) *EMBO J.* **11**, 4787–4794
 29. Sirrenberg, C., Bauer, M. F., Guiard, B., Neupert, W., and Brunner, M. (1996) *Nature* **384**, 582–585
 30. Kovermann, P., Truscott, K. N., Guiard, B., Rehling, P., Sepuri, N. B., Muller, H., Jensen, R. E., Wagner, R., and Pfanner, N. (2002) *Mol. Cell* **9**, 363–373
 31. Luciano, P. V. S., Vergnolle, M. A., Dyal, S. D., Robinson, D. R., and Tokatlidis, K. (2001) *EMBO J.* **20**, 4099–4106
 32. Koehler, C. M., Murphy, M. P., Bally, N. A., Leuenberger, D., Oppliger, W., Dolfini, L., Junne, T., Schatz, G., and Or, E. (2000) *Mol. Cell Biol.* **20**, 1187–1193
 33. Kerscher, O., Holder, J., Srinivasan, M., Leung, R. S., and Jensen, R. E. (1997) *J. Cell Biol.* **139**, 1663–1675
 34. Kerscher, O., Sepuri, N. B., and Jensen, R. E. (2000) *Mol. Biol. Cell* **11**, 103–116
 35. Tokatlidis, K., and Schatz, G. (1999) *J. Biol. Chem.* **274**, 35285–35288
 36. Endres, M., Neupert, W., and Brunner, M. (1999) *EMBO J.* **18**, 3214–3221
 37. Curran, S. P., Leuenberger, D., Oppliger, W., and Koehler, C. M. (2002) *EMBO J.* **21**, 942–953
 38. Stafford, W. F., III (1992) *Anal. Biochem.* **203**, 295–301
 39. Azem, A., Oppliger, W., Lustig, A., Jenö, P., Feifel, B., Schatz, G., and Horst, M. (1997) *J. Biol. Chem.* **272**, 20901–20906
 40. Sheehan, J. K., Howard, M., Richardson, P. S., Longwill, T., and Thornton, D. J. (1999) *Biochem. J.* **338**, 507–513
 41. Thornton, D. J., Howard, M., Khan, N., and Sheehan, J. K. (1997) *J. Biol. Chem.* **272**, 9561–9566
 42. Rost, B. (1996) *Methods Enzymol.* **266**, 525–539
 43. King, R. D., and Sternberg, M. J. (1996) *Protein Sci.* **5**, 2298–2310
 44. Dempsey, B. R., Economou, A., Dunn, S. D., and Shilton, B. H. (2002) *J. Mol. Biol.* **315**, 831–843
 45. Bauer, M. F., Hofmann, S., Neupert, W., and Brunner, M. (2000) *Trends Cell Biol.* **10**, 25–31
 46. Frydman, J., Nimmesgern, E., Ohtsuka, K., and Hartl, F. U. (1994) *Nature* **370**, 111–117
 47. Langer, T., Lu, C., Echols, H., Flanagan, J., Hayer, M. K., and Hartl, F. U. (1992) *Nature* **356**, 683–689
 48. Schroder, H., Langer, T., Hartl, F. U., and Bukau, B. (1993) *EMBO J.* **12**, 4137–4144
 49. Szabo, A., Korszun, R., Hartl, F. U., and Flanagan, J. (1996) *EMBO J.* **15**, 408–417
 50. Schleiff, E., Shore, G. C., and Goping, I. S. (1997) *J. Biol. Chem.* **272**, 17784–17789
 51. Schlossmann, J., Dietmeier, K., Pfanner, N., and Neupert, W. (1994) *J. Biol. Chem.* **269**, 11893–11901
 52. Smagula, C. S., and Douglas, M. G. (1988) *J. Cell. Biochem.* **36**, 323–327
 53. Wiedemann, N., Pfanner, N., and Ryan, M. T. (2001) *EMBO J.* **20**, 951–960
 54. Miroux, B., and Walker, J. E. (1996) *J. Mol. Biol.* **260**, 289–298